

Application of Biomass Energy Monitoring Based on Renewable Energy Supply in Sports

Yaodong Ding¹

¹ Department of Physical Education, ChangSha Normal University
Changsha, China

E-mail: dingyaodong1990@163.com

Abstract. Biomass energy is an ideal form of clean, renewable energy, characterized by its wide availability, low cost, strong renewability, and minimal pollution. The development and utilization of biomass energy are crucial for mitigating greenhouse effects, reducing air pollution, and alleviating energy pressure. Multi-functional biomass energy monitoring equipment and integrated systems have received extensive attention and are flourishing. This integrated design demonstrates a higher degree of integration, overall unity, diversification, and intelligence, which helps overcome the current developmental challenges of single-functionality and system isolation. One of the most representative designs of these integrated devices is the multi-energy conversion and utilization system, which efficiently converts low-grade energy into high-grade energy and provides various conversion pathways within a single system. This supplies ample energy for daily life and enables its full application in sports. By integrating self-powered wearable technology, this paper explores the use of a wearable sensor composed of KAP composite polyacrylamide/polyacrylic acid hydrogel (PAAH), namely KAP PAAH. The strain-voltage response and real-time sensing provided by KAP PAAH facilitate an electrically driven, self-powered integrated wearable sensor for human joint health monitoring. Additionally, this approach maximizes the residual value of biomass waste, highlighting its potential and high economic value for future practical applications. Specifically, the optimized design ensures reliable and continuous health monitoring during various sports activities, thus aligning with the broader environmental benefits of biomass energy.

Key words. Renewable Energy, Biomass, Sports, Monitoring.

1. Introduction

As society progresses and develops, the main issues hindering people's advancement are resource scarcity and energy crises, with freshwater scarcity being one of the severe problems facing human survival. Water is one of the most abundant resources on Earth, but most of it is seawater, which cannot be utilized by humans due to its high salinity [1], [2], [3]. Therefore, the development and implementation of large-scale, efficient seawater desalination technologies is urgently needed. Solar energy, as a sustainable and environmentally friendly energy source, has been the focus of scientists in recent years [4], [5]. Solar-driven water evaporation, a common natural

phenomenon, is an integral part of the Earth's water cycle and offers advantages such as low manufacturing costs, simple processes, ease of use, promising prospects, and environmental friendliness.

Wearable physiological monitoring systems are technologies capable of detecting various stimuli and producing accurate responses. With the rapid development and progress of society, people enjoy the conveniences brought by technological advancements in daily life. Monitoring one's health status during physical activities has become a focus of attention. Consequently, many researchers are dedicated to developing wearable health monitoring sensors that can monitor health conditions in real-time during physical activities, providing immediate warnings and reminders for timely medical treatment [6], [7], [8]. The exploration and development of flexible, wearable health sensors for real-time monitoring and feedback of joint health during physical activities are imperative. Moreover, achieving self-powered integration in wearable sensors to solve the power supply issue is a priority in research.

Benefiting from excellent energy conversion efficiency, good conductivity, and flexible sensing capabilities, multifunctional device-level integrated systems have recently gained immense popularity and development. This all-in-one design represents a higher degree of integration, facilitating the creation of devices with more compatible and intelligent functions, thereby addressing the current limitations of single-functionality and limited capabilities [9], [10], [11]. The convergence of wearable sensor technology, flexible electronics, power sources, and energy conversion technologies offers new opportunities for enhancing health analysis levels, conducting real-time physiological monitoring, and building and transmitting health big data. This shift in focus towards the research and development of photothermal materials paves the way for effective utilization of various materials in developing multifunctional device-level integrated technologies [12], [13]. By synthesizing and manipulating the structures of materials and optimizing the design and construction of devices, there is potential to integrate energy conversion/storage systems, personal thermal management,

flexible power sources, and wearable sensors for health monitoring, providing practical application value.

This paper investigates the changes in surface structure of different biomasses, such as pomelo peel, peanut shells, and corn stalks, activated by three methods: KOH, K₂FeO₄, and C₃H₆N₆. It studies their light absorption, water vapor generation, and thermal management to enhance their photothermal conversion efficiency. Additionally, leveraging the excellent photothermal conversion capability of solar-driven water evaporation, this paper presents an alternative method for generating the most widely used form of energy in practical applications: electricity. By using thermoelectric generators to convert solar energy into thermal energy and subsequently into electrical energy, this method is used to create wearable sensors for health monitoring during physical activities.

2. Methodology

A. Wearable Sensor Development

The wearable sensor is composed of KAP composite polyacrylamide/polyacrylic acid hydrogel (PAAH), known as KAP PAAH. The development process involves the synthesis of KAP PAAH, where 1.53g of acrylamide and 0.47ml of acrylic acid are added to deionized water and stirred for 5 minutes. Subsequently, 0.12g of sodium carboxymethyl cellulose and 0.03g of KAP photothermal material are mixed into the solution, followed by the addition of ammonium persulfate. The mixture is then heated to 70°C in an oven for 2 hours, resulting in the formation of KAP-loaded polyacrylamide/polyacrylic acid composite hydrogel.

B. Activation Methods for Biomass

The activation of biomass is conducted using three different methods: KOH, K₂FeO₄, and melamine. Activation with KOH: Pomelo peels, corn stover, and peanut shells are washed, dried, and soaked in 1M KOH solution for 10 hours. The soaked biomass is dried, ground into powder, and carbonized at 600°C for 2 hours in a muffle furnace. The carbonized powders undergo hydrophilic treatment using a mixed acid of VH₂SO₄ =3:1 for 12 hours, washed until pH=7, and dried for future use.

Activation with K₂FeO₄: Carbonized corn stover, pomelo peels, and peanut shells are soaked in 0.1M K₂FeO₄ solution for 9 hours, dried at 100°C, and re-carbonized at 600°C for 2 hours. The powders are then hydrophilically treated similarly to the KOH activation method.

Activation with Melamine: The biomass powders are mixed with melamine and deionized water, stirred, and freeze-dried. The freeze-dried powders are carbonized at 600°C for 2 hours and hydrophilically treated as described above.

C. Experimental Design and Controls

To ensure the validity and reproducibility of the results, several control setups were implemented:

Control Setup 1: Unactivated biomass powders were used as a control to compare the effects of different activation methods.

Control Setup 2: Thermoelectric generators without any photothermal material coating were used to measure baseline power generation under solar irradiation.

Control Setup 3: Different mass loads (0.01g, 0.03g, 0.05g) of KAP were tested to determine the optimal load for maximum water evaporation rate and photothermal conversion efficiency.

D. Parameters Measured

The following parameters were measured during the experiments:

Strain-Voltage Response: Measured to evaluate the sensor's ability to monitor joint health.

Real-Time Sensing Monitoring: Assessed to verify the sensor's functionality in providing continuous health monitoring.

Water Evaporation Rate: Monitored to determine the efficiency of photothermal conversion.

Output Voltage of Thermoelectric Generators: Recorded to evaluate the power generation performance of different biomass carbon coatings.

Resistance Changes in Sensors: Analyzed during tensile, bending, and compression tests to assess the sensor's mechanical and temperature responsiveness.

E. Preparation of Photovoltaic Devices

Wood pulp paper is cut to the desired size, then 0.075 g/cm² of KAP biomass carbon material is coated on the paper, followed by drying in an oven. After drying, the carbon paper is placed in a plasma cleaner for oxygen ion plasma treatment. White cotton cloth, beige cotton cloth, and aloe cloth are cut to the desired size and hydrophilically treated by heating in a concentrated detergent solution at 100°C for 30 minutes, then dried in an oven. The dried cotton cloths are then ultrasonicated in a mixture of KAP biomass carbon material and anhydrous ethanol. After a certain duration of ultrasonication, the carbon cloths loaded with KAP biomass carbon material are dried in an oven, coated on the paper, and then dried in the oven again.

3. Results and Discussion

A. Biomass Photothermal Conversion Photothermal Conversion Effects of Different

1) Biomasses Under Various Activation Methods

Morphological images of biomasses treated with different activation methods are shown in Figure 1. After various

activation methods, different biomasses essentially retain their original structures while developing new microstructural features. Compared to the unactivated biomass raw powders (Figure 2), the pomelo peels activated by different methods retain their inherent porous structure. Among the three activation methods, KOH activation is the most effective, creating interconnected honeycomb-like pores with a diameter of about 1 μm , providing robust support for water transport. Pomelo peels activated with K_2FeO_4 and $\text{C}_3\text{H}_6\text{N}_6$ exhibit circular pores of about 2 μm on their surfaces but do not form a three-dimensional interconnected pore structure. The circular pores generated by K_2FeO_4 activation are relatively uniform in size and evenly distributed.

The peanut shells activated with KOH develop fine and interconnected three-dimensional pore structures. After K_2FeO_4 and melamine activation, the peanut shells retain their original row-like structure and form pores of various sizes on the surface. Melamine-activated shells develop about 3 μm pores on their sides, providing effective channels for water transport. Corn stover, after the three types of activation, retains its three-dimensional bundle structure well. The sides of corn stover activated with K_2FeO_4 develop pores that absorb water, ensuring effective water transport and evaporation.

Before activation, the surfaces of all three biomasses are relatively smooth. Compared to the unactivated raw powders and unactivated biomass carbon powders, the activated biomass carbons exhibit many more surface pores, forming three-dimensional porous structures that provide favorable conditions for light absorption and effective water transport. The peanut shells and corn stover inherently possess two-dimensional bundle channel structures with smaller and fewer pores on the tube walls [14], [16]. The pomelo peels activated with KOH, which have larger pore diameters than peanut shells and corn stover, exhibit a three-dimensional cheese-like pore structure, interconnected, ensuring the absorption of sunlight and water transport.

Additionally, grinding the biomass before activation and carbonization, as opposed to the approach of other researchers who carbonize whole biomasses such as radish, magnolia fruit, mushrooms, and sugarcane, offers higher flexibility. This method retains the structural features of the biomass while allowing for stacking, creating more pore structures to enhance sunlight absorption and facilitate water transport, thereby improving the efficiency of solar photothermal conversion.

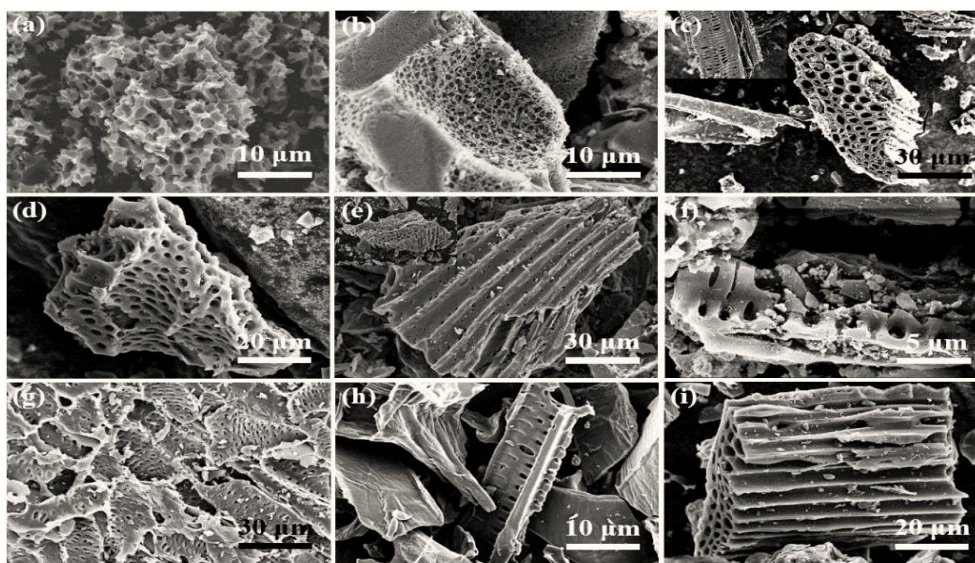


Figure 1. (a) KOH Activated Pomelo Peels; (b) KOH Activated Peanut Shells; (c) KOH Activated Corn Stalks; (d) K_2FeO_4 Activated Pomelo Peels; (e) K_2FeO_4 Activated Peanut Shells; (f) K_2FeO_4 Activated Corn Stalks; (G) Melamine Activated Pomelo Peels; (h) Melamine Activated Peanut Shells; (i) Melamine Activated Corn Stalks

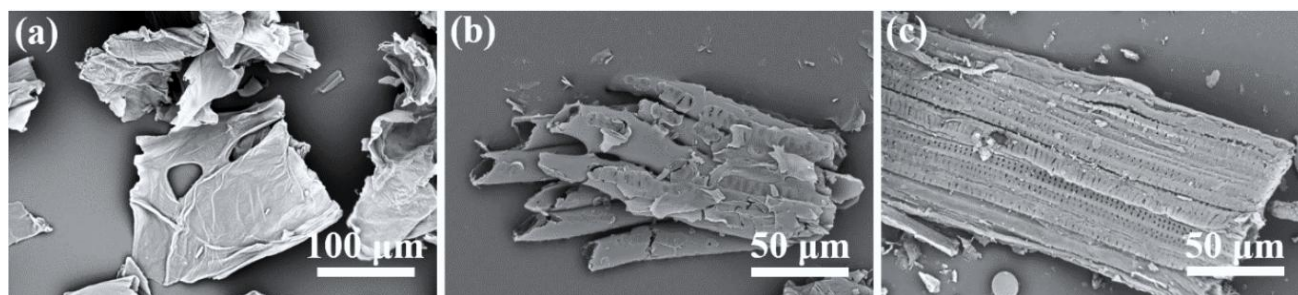
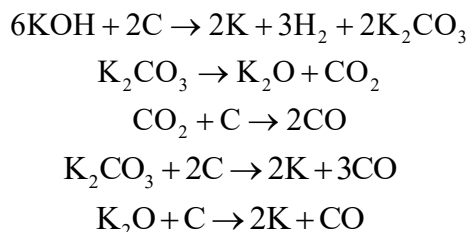


Figure 2. SEM Images of Various Biomass Without Activation And Carbonization: (a) Pomelo Peels; (b) Peanut Shells; (c) Corn Stalks

Due to the significant structural changes in biomass before and after activation, we investigated the activation mechanisms corresponding to the three methods. During the KOH activation process, the reaction initiates as a solid-solid reaction, followed by a solid-liquid reaction [15], [16], [17]. This includes the reduction of potassium compounds to form metallic K, oxidation of carbon to CO/CO₂ and carbonates, and other reactions among various active intermediates. In both physical and chemical activation processes, the carbon lattice irreversibly expands, resulting in a high microporosity.



In the K₂FeO₄ activation process, K₂FeO₄ serves both as an activating agent (K) and as a catalyst (Fe) to achieve simultaneous carbonization and graphitization of the biomass. The activation with KOH and catalysis by Fe species are carried out in the following reactions, but not necessarily in sequence.

2) Impact of Load Amount and Device Design on Solar Photothermal Conversion Efficiency

The selection of photothermal materials and the design of water evaporation devices are particularly crucial for solar water evaporation experiments. Therefore, we delved deeper into aspects such as the load amount of

photothermal materials on the substrate and changes in device design. Focusing on KAP, which has the most outstanding photothermal conversion performance and a honeycomb-cheese-like structure, an insulating layer and a water transport device made of PS foam and gauze were used. When the load amounts were 0.01g, 0.03g, and 0.05g respectively (Figure 3(a-b)), their evaporation rates reached 1.59 kg·m⁻²·h⁻¹, 1.64 kg·m⁻²·h⁻¹, and 1.62 kg·m⁻²·h⁻¹, with corresponding photothermal conversion efficiencies of 88.4%, 92.6%, and 90.5%. This indicates that the load amount is not simply a case of 'the more, the better'; rather, there is an optimal value, which in this case is 0.03g, where the water evaporation rate is maximized. This is because at 0.01g, there is too little photothermal material on the paper, allowing only limited photothermal conversion and water evaporation. At 0.05g, the photothermal material is overly saturated, densely packed, and blocks some water escape channels, leading to a decrease in both evaporation rate and photothermal conversion efficiency compared to a load of 0.03g.

Moreover, as shown in Figure 3(c), the surface temperature of the photothermal material at a load of 0.03g is actually the lowest compared to 0.01g and 0.05g. This is because thermal radiation is directly proportional to the fourth power of temperature ($\phi = \varepsilon A \sigma (T_1^4 - T_2^4)$), where ϕ is the heat flux, ε is the emissivity, A is the surface area, σ is the Stefan-Boltzmann constant, and T_1 and T_2 are the working temperature of the interface and the ambient temperature, typically room temperature). Thus, the higher the surface temperature, the greater the thermal radiation and heat loss. Therefore, a lower surface temperature results in reduced thermal radiation between the interface and the surrounding environment.

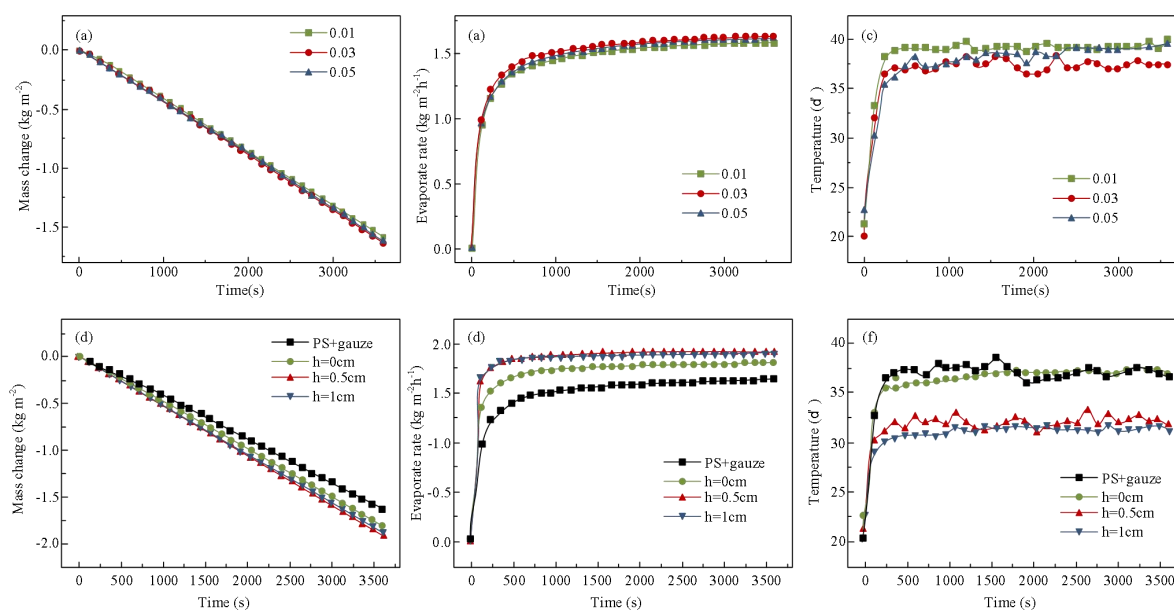


Figure 3. Mass Change, Evaporation Rate and Temperature Changes Test Results of (a-c) Different Mass Loads of KAP, (d-f) Different Devices

When using an insulating device made of PS foam and gauze, some heat is conducted to the gauze, resulting in heat loss. To address this, we switched to a design

combining a cotton tube with PS foam. This new design minimizes contact between the photothermal material, insulating layer, and water transport layer, significantly

reducing heat loss through conduction. We also explored how varying the protruding height of the cotton tube affects water evaporation rates. According to experimental results (Figure 3(d-f)), the water evaporation rates at cotton tube heights of 0 cm, 0.5 cm, and 1 cm were $1.81 \text{ kg}\cdot\text{m}^{-2}\cdot\text{h}^{-1}$, $1.95 \text{ kg}\cdot\text{m}^{-2}\cdot\text{h}^{-1}$, and $1.89 \text{ kg}\cdot\text{m}^{-2}\cdot\text{h}^{-1}$, respectively. The cotton tube system effectively reduces thermal loss by decreasing the contact area between the substrate material and the insulating layer.

The optimal height for the cotton tube system was found to be 0.5 cm. Temperature changes indicated that as the cotton tube's protruding height increased, the system's surface temperature decreased. The best evaporation rate was obtained at a height of 0.5 cm, where the system's temperature dropped from 36°C to 32.1°C , with the temperature at the center of the photothermal material as the reference. Under the same illuminated area, the increased contact area between the device and air provided more escape channels for the evaporated water. Additionally, as the system temperature decreased, thermal radiation loss between the entire evaporation system and the external environment was reduced, thereby improving the evaporation rate and photothermal conversion efficiency. However, when the protruding height increased from 0.5 cm to 1 cm, the evaporation rate and conversion efficiency actually decreased despite no change in the illuminated and water evaporation areas. The system temperature changed marginally from 32.1°C to 31.3°C ,

causing minimal variation in thermal radiation to the external environment. We speculate that the increased distance between the paper loaded with photothermal material and the water-storing beaker and PS foam below provided more space for heat dissipation, leading to reduced evaporation rates and conversion efficiency.

3) Thermoelectric Power Generation with Biomass Carbon Powders

To enhance energy utilization, we applied various biomass carbon powders as coatings on thermoelectric generators. As shown in Figure 4 (a-b), when equal amounts of different biomasses are coated on thermoelectric generators, their power generation capabilities vary due to differences in light absorption and photothermal conversion abilities. For different biomasses activated with KOH, such as KAP, peanut shells, and corn stover, the output voltages in thermoelectric generation are 197 mV, 135 mV, and 133 mV, respectively. Meanwhile, the same biomass, pomelo peel, activated differently with KOH, K_2FeO_4 , and melamine, exhibits output voltages in thermoelectric generation of 197 mV, 156 mV, and 145 mV, respectively. This indicates that the photothermal conversion performance of various biomasses, post-activation and carbonization, differs due to the distinctiveness of their microstructures.

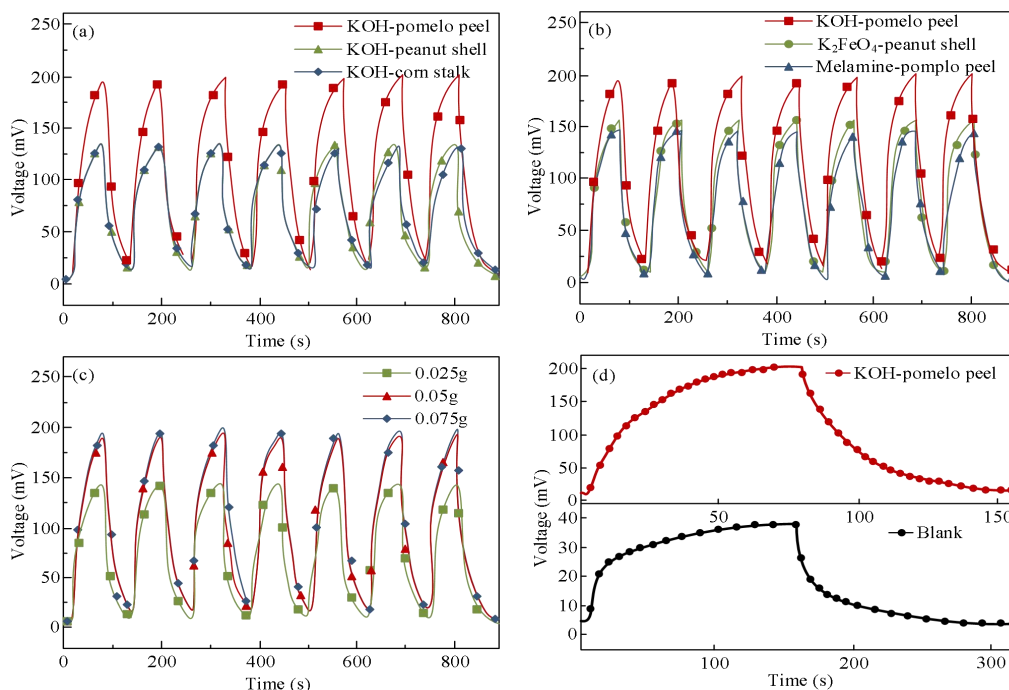


Figure 4. Comparison of Voltage Output Signals of Thermoelectric Power Generation, (a) KOH Activates Different Biomass; (b) Different Activation Methods of Pomelo Peels; (c) Different Mass Loads of KAP; (d) Comparison of Power Generation Performance between KAP and Blank Thermoelectric Power Generation Sheet

When examining the solar photothermal conversion performance of biomass, we found that the water evaporation rate and photothermal conversion efficiency varied with different amounts of biomass carbon. We hypothesized that the power generation performance would also differ when coating thermoelectric generators with

varying amounts of biomass carbon material. Based on previous experimental results, we selected KAP biomass carbon, which showed the best power generation performance, for further study. We coated the thermoelectric generators with 0.025g, 0.05g, and 0.075g of KAP. As shown in Figure 4(c), the power generation at

these load amounts was 142 mV, 186 mV, and 197 mV, respectively. Increasing the load from 0.025g to 0.05g resulted in a 30.9% rise in power generation, from 142 mV to 186 mV. However, further increasing the load to 0.075g only produced a 5.9% increase, from 186 mV to 197 mV. Considering material efficiency, we determined that 0.05g is the optimal load amount. Comparing a blank thermoelectric generator without any photothermal material to one coated with KAP, we found that the blank generator produced 38 mV under solar irradiation, while the KAP-coated one generated 197 mV. This significant improvement highlights KAP's exceptional photothermal conversion ability.

B. Biomaterials for Flexible Wearable Sports Health Monitoring

1) Basic Performance

Before monitoring human joint health, we conducted a series of basic performance tests on the prepared KAP PAAH, including tensile, bending, compression properties, and temperature sensing. In the tensile test of KAP PAAH (Figure 5(a)), we stretched the KAP PAAH with deformations of 5 mm, 10 mm, and 15 mm. Due to the varying amounts of deformation, the sensor's resistance increased with the deformation, and it maintained stable resistance values even after multiple stretch-recovery cycles at different lengths. This indicates that our wearable sensor exhibits good cyclic stability, a critical feature for practical applications. For the sensitivity test of wearable sensors, the gauge factor (GF) is an important parameter. The gauge factor is defined as:

$$GF = \frac{dX}{\varepsilon} \quad (1)$$

dX represents the relative change in resistance, and is ε the applied strain. When our prepared KAP PAAH sensor was

stretched by 5mm, 10mm, and 15mm, the corresponding resistance changes were relatively uniform, with a gauge factor of 8000. For this type of strain-resistive sensor, its internal working mechanism primarily involves changes in resistance due to structural deformation of the sensor. For example, the spacing between photothermal components changes due to the applied strain, and the stretching strain causes the gaps between KAP particles to widen and the cross-sectional area to decrease, resulting in increased resistance.

When conducting bending (Figure 5(b)) and compression experiments (Figure 5(c)) on KAP PAAH, the material also showed good responses. When KAP PAAH was folded and bent, the resistance increased, and when it was restored to its original state, the resistance decreased. The performance remained stable throughout, indicating strong practical application value and prospects. We also conducted temperature response experiments on KAP PAAH (Figure 5(d-e)). The results indicate that as the temperature increases, the current through KAP PAAH increases and the resistance decreases. Conversely, as the temperature decreases, the resistance increases. The sensor showed good temperature responsiveness. As the temperature linearly increased, the decrease in resistance was initially rapid and then slowed down, following the same pattern during temperature decrease. This is because, during the experiment, as the gel was exposed to sunlight for longer periods and water loss increased, the resistance increased. This is due to water molecules being electrolytes, but their ionization degree at room temperature is minimal and almost negligible, meaning there are few free-moving ions. However, at higher temperatures, many water molecules ionize into H^+ and OH^- , leading to more free charges. Additionally, the polyacrylic acid in the gel also ionizes. As the temperature rises, H^+ ions from $-COOH$ groups ionize further, leading to a decrease in resistance.

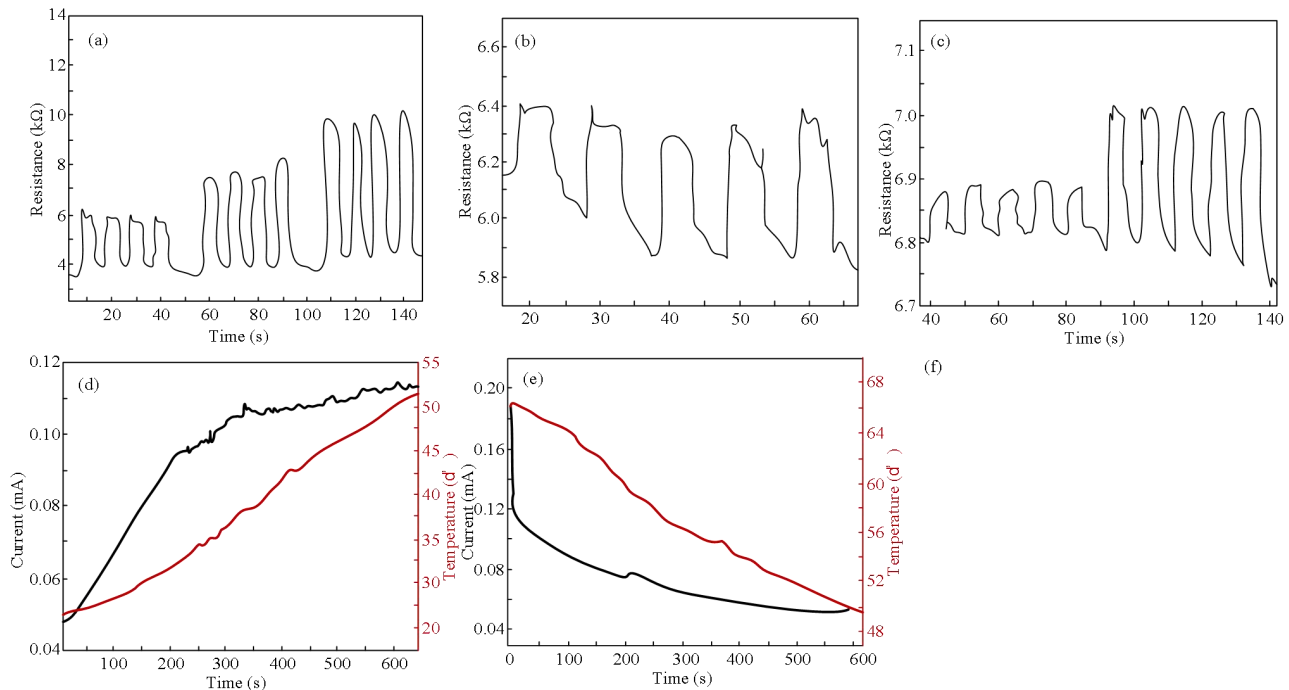


Figure 5. KAP PAAH Performance Test Results of (a) Tensile Performance; (b) Bending Performance; (c) Compression Performance; (d-e) Temperature Induction

2) KAP PAAH for Monitoring Joint Health in Sports Activities

A tendon sheath is a double-layered, enclosed synovial tube that surrounds the tendon, serving as a protective and lubricating cover. It consists of two layers encasing the tendon, with a synovial cavity in between containing synovial fluid. The inner layer adheres closely to the tendon, while the outer layer lines the inside of the fibrous sheath. Together, they combine with the bone surface to fix, protect, and lubricate the tendon, preventing friction or compression damage. Long-term excessive friction can cause inflammatory damage to the tendon and sheath, leading to swelling known as tenosynovitis. Types of tenosynovitis include radial styloid stenosing tenosynovitis, flexor tendon stenosing tenosynovitis, and ulnar side wrist extensor tendon sheath inflammation. Primary symptoms include radial side wrist pain, impaired thumb mobility, snapping and pain during finger movement, and wrist weakness when exerted. If untreated, it may lead to permanent movement restrictions. Early-stage tenosynovitis usually shows no symptoms, only becoming

painful as it progresses, making regular monitoring of finger and wrist joints essential in daily life.

After testing the basic properties of KAP PAAH, we found it has excellent shape plasticity, compressibility, and a stable strain-resistance response. These characteristics make it well-suited for monitoring joint health during physical activities. The flexible wearable sensors we developed can monitor joint health in real-time during movement and provide timely reminders for medical attention when needed. For healthy and flexible finger joints, the sensor can sensitively detect resistance changes during rapid bending and straightening. When the joint bends quickly, the sensor detects a rapid increase in resistance. When the joint maintains a bent position without change, the resistance remains constant. As the joint quickly returns to a straight position, the resistance rapidly decreases, returning to its original value. After multiple testing cycles, the resistance signal remains stable, demonstrating the sensor's excellent cyclic stability.

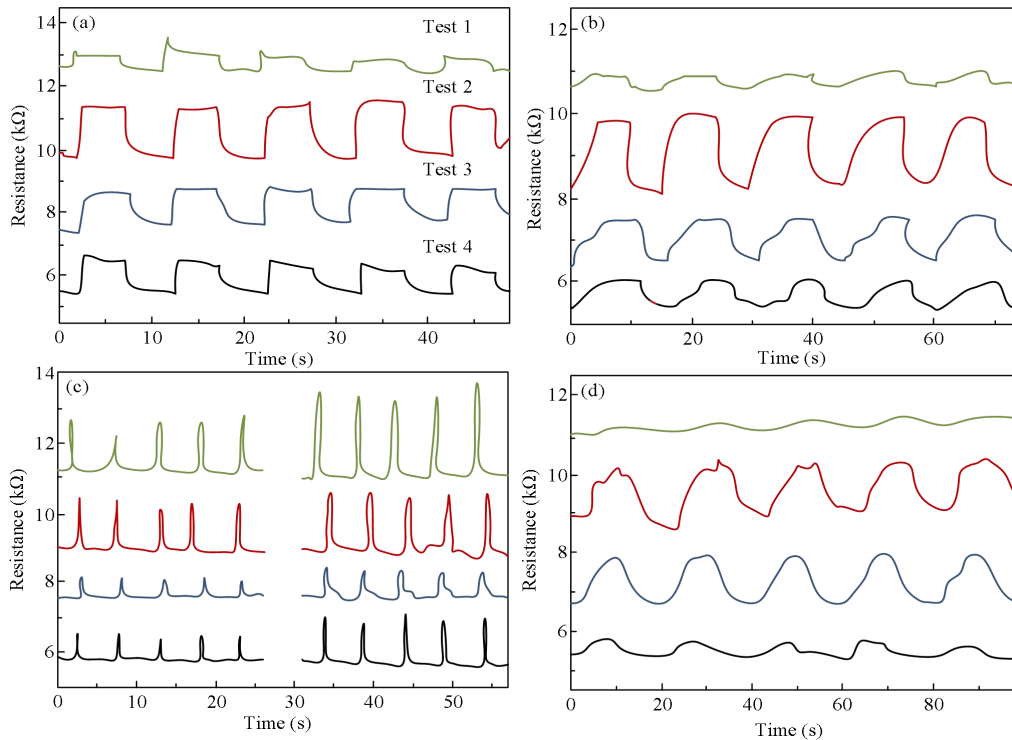


Figure 6. Comparison of the Results of Sensor Resistance Changes in Different Movement States of Knuckles (a) Finger Joints Bend and Straighten Quickly; (b) Finger Joints Bend Slowly and Straighten Quickly; (c) Finger Joints Bend 45° and 90°; (d) Finger Joints Bend and straighten Slowly

C. Discussion

The successful development and application of the integrated multi-energy conversion and utilization system, along with the KAP PAAH wearable sensor, have significant implications for both renewable energy utilization and health monitoring in sports. The efficient conversion of low-grade energy into high-grade energy within a single system underscores the potential of biomass energy as a sustainable alternative to conventional energy sources, applicable in various fields beyond sports, such as

residential energy systems and portable electronic devices. The integration of self-powered wearable sensors into sports health monitoring systems offers a novel approach to real-time physiological monitoring, with the KAP PAAH sensor demonstrating high sensitivity and stability, making it effective for preventing injuries, optimizing performance, and enhancing overall athlete health management. However, the study has limitations, including the focus on specific biomass materials and the controlled laboratory conditions that may not fully replicate real-world scenarios. Future research should explore a wider

range of biomass sources, conduct field tests to validate the findings, and optimize the system design for enhanced performance and broader applications. By addressing these areas, the study provides a foundation for developing advanced, multifunctional devices that can significantly impact various fields, contributing to a more sustainable and health-conscious future.

4. Conclusion

In today's society, amidst economic growth and rapid societal development, energy crises and resource shortages have become severe issues impacting people's normal lives. Addressing these challenges and efficiently developing and utilizing renewable energy have emerged as critical tasks. The multifunctional device-level integrated system, characterized by its integrative, diverse, and intelligent nature, offers a promising solution to these challenges, helping to overcome the current limitations of single-functionality and system isolation. These integrated devices facilitate the versatile conversion of low-grade energy into high-grade energy within a single system, providing diverse conversion pathways to ensure ample energy supply for people's daily needs. Biomass carbon materials, with their excellent porous structure, also find significant applications in wearable sports health sensing and monitoring. The main conclusions of the article are:

(1) Biomass carbon materials, after activation and high-temperature treatment, retain their original skeletal structure while incorporating numerous pore structures, creating a three-dimensional porous structure. This provides strong support for light absorption and water transport. Additionally, by varying the water evaporation device and load amounts, we further explored the impact of thermal management and load quantity on solar photothermal conversion efficiency. It was found that the overall conversion efficiency of the cotton tube device is higher than the PS+gauze device, and the highest photothermal conversion efficiency of 1.95 kg m⁻² h⁻¹ is achieved at a cotton tube protrusion height of 0.5 cm, with minimal heat loss. The optimal load amount is 0.03g, corresponding to a water evaporation rate of 1.64 kg m⁻² h⁻¹.

(2) Due to the excellent conductive properties of biomass carbon materials, when mixed with polyacrylamide/polyacrylic acid hydrogel, a wearable health monitoring sensor with superior conductivity is produced. This sensor can flexibly monitor the flexibility of joint movements and the presence of discomfort during physical activities. The real-time feedback on joint movement greatly assists users in understanding their joint health status during exercise.

References

[1] K. A. M. İ. L. Kaygusuz and S. E. D. A. T. Keleş, "Use of biomass as a transitional strategy to a sustainable and clean energy system," *Energy Sources, Part A: Recovery, Utilization, and Environmental Effects*, vol. 31, no. 1, pp. 86-97, 2008.

[2] K. Wang et al., "Flexible PVT-ORC hybrid solar-biomass cogeneration systems: The case study of the University Sports

Centre in Bari, Italy," in *The 5th International Seminar on ORC Power Systems, Athens, Greece*, pp. 9-11, Sep. 2019.

[3] Y. Sun, Y. Z. Li, and M. Yuan, "Requirements, challenges, and novel ideas for wearables on power supply and energy harvesting," *Nano Energy*, vol. 115, p. 108715, 2023.

[4] Y. Zhang et al., "Wearable thermoelectric cooler based on a two-layer hydrogel/nickel foam heatsink with two-axis flexibility," *ACS Applied Materials & Interfaces*, vol. 14, no. 13, pp. 15317-15323, 2022.

[5] S. E. Dijkema, "The interpretative flexibility of smart wearables. A critical reflection on the promise of smart wearable technology," (Master's thesis), 2016.

[6] Z. Liu et al., "Towards wearable electronic devices: A quasi-solid-state aqueous lithium-ion battery with outstanding stability, flexibility, safety and breathability," *Nano Energy*, vol. 44, pp. 164-173, 2018.

[7] P. Rytka, "Wearable Heart Rate Monitor with Additional Flexibility," *Sensor technology: Detection, Monitoring and Measurement Insights*, vol. 2011, no. 12, p. 27, 2011.

[8] C. L. Kim et al., "Smart wearable heaters with high durability, flexibility, water-repellent and shape memory characteristics," *Composites Science and Technology*, vol. 152, pp. 173-180, 2017.

[9] E. S. Lora and R. V. Andrade, "Biomass as energy source in Brazil," *Renewable and Sustainable Energy Reviews*, vol. 13, no. 4, pp. 777-788, 2009.

[10] Z. Liu, "Decision-making for biomass-based production chains: The basic concepts and methodologies," vol. 258. ISBN: 978-0-12-814278-3, 2020.

[11] L. R. Amjith, and B. Bavanish, "A review on biomass and wind as renewable energy for sustainable environment," *Chemosphere*, vol. 293, p. 133579, 2022.

[12] R. Liu et al., "Novel investigation of pyrolysis mechanisms and kinetics for functional groups in biomass matrix," *Renewable and Sustainable Energy Reviews*, vol. 153, p. 111761, 2022.

[13] T. A. Volk et al., "Greater potential for renewable biomass energy," *BioScience*, vol. 53, no. 7, pp. 620-621, 2003.

[14] Y. Kun et al., "Thermodynamic analysis of biomass and natural gas fueled distributed energy system (BNDES)," *Chemical Engineering (China)*, 2016.

[15] X. Zhao et al., "Biomass-based chemical looping technologies: the good, the bad and the future," *Energy & Environmental Science*, vol. 10, no. 9, pp. 1885-1910, 2017.

[16] G. J. Herbert and A. U. Krishnan, "Quantifying environmental performance of biomass energy," *Renewable and Sustainable Energy Reviews*, vol. 59, pp. 292-308, 2016.

[17] M. I. Muhamad et al., "Optimal design of hybrid renewable energy system based on solar and biomass for halal products research institute, UPM," in *2014 IEEE Innovative Smart Grid Technologies-Asia (ISGT ASIA)*, pp. 692-696, May. 2014.